CHAPTER 5

ADSORPTION OF METHYLENE BLUE ONTO THE ACTIVATED CARBON TREATED WITH HYDROCHLORIC ACID

5.1 Introduction

Activated carbons prepared from agricultural by-products and wastes were reported to result in highly porous carbon structure (Yahya et al., 2015). However, surface modifications and restructuring of the carbon molecules are among the techniques used to optimize the adsorption capacity by the activated carbon (Lee et al., 2016).

Acid treatment process is one of the process of optimization. This process involves demineralize of the carbon from the unwanted minerals as the acid removes the inorganic species from the prepared activated carbon's surfaces. At the end of the treatment, the purity, surface area, and porosity of the activated carbon are increased (Liou & Wu, 2010).

The purpose of this work was to investigate the performance of the prepared activated carbon treated with hydrochloric acid in removal of methylene blue from aqueous solution using batch equilibrium tests, adsorption isotherm and adsorption kinetics studies.

5.2 Materials

The adsorbent (CNAC-D3) used was the prepared activated carbon from cocoa nibs (CNAC-800-3) which was initially activated at 800 °C and impregnated with K_2CO_3 at impregnation ratio of 3:1. All chemical reagents used in this work were procured from the Merck, Malaysia (hydrochloric acid 30%), Essex, UK (sodium hydroxide 99 %) and Hamburg Chemical GmbH (Methylene blue in powder form).

5.3 Methods

Batch equilibrium studies were carried out for adsorption of methylene blue on the treated activated carbons (CNAC-D3). The effects of initial adsorbate concentration, solution pH and contact time on the adsorption uptake and percentage removal were investigated. The stock solution (1000 mg/L) of methylene blue was prepared prior experiments.

In order to prepare 1000 mg/L of methylene blue solution, approximately 1.0 gram of methylene blue (powder) was weighed and transferred into 1000 mL of volumetric flask. About 1000 mL of deionised water was added to mark. The absorbance of methylene blue concentration was determined at 668 nm using a UV-Vis spectrophotometer. The calibration curve was obtained from the spectra of the standard solutions (5 - 100 ppm).

The stock solution was stored in dark place to prevent direct sunlight to avoid decolourization and degradation. All chemical wastes were collected in proper containers before disposal.

The sample solutions were withdrawn at equilibrium to determine the residual concentration. The amount of adsorbate adsorbed, q_e (mg/g) and the percent removal of

adsorbate at equilibrium was calculated according to Equation 4.1 and Equation 4.2 (as presented in Chapter 4).

5.3.1 Effect of Initial Adsorbate Concentration

The effects of initial methylene blue concentration were studied on the adsorption capacity and percent removal. Approximately, 200 mL of methylene blue solutions with known initial concentration (25-100 mg/L) were prepared in a series of 250 mL Erlenmeyer flasks. The amount of adsorbent that was added into each flask containing the adsorbates was fixed at 0.1 g. The opening of the flasks were sealed with parafilm and the flasks were then placed in an isothermal water bath shaker at constant temperature (30 °C), with rotation speed of 120 rpm, until equilibrium point was reached.

5.3.2 Effect of solution pH

The effect of solution pH was studied on the adsorption capacity using different initial pH of the solutions, ranged from 2 to 9. Hydrochloric acid (0.1 M) and sodium hydroxide (0.1 M) was used to adjust the pH. The initial concentration was 100 mg/L for each flask and was added with 0.1 g of adsorbent. The solution temperature was at 30 °C.

5.4 Results and Discussion

5.4.1 Effect of Initial Concentration

Figure 5.1 shows the effects of initial concentrations on the adsorption of methylene blue onto cocoa nib-based activated carbons (acid treated – CNAC-D3, and untreated – CNAC-800-3). The initial concentrations were set at 25, 50, 100, 200, 300,

400 and 500 mg/L. It can be easily observed that the adsorption capacity of methylene blue on both activated carbons was increased as the initial concentrations increased. The trend for both activated carbons was almost alike as they possess high surface areas (more than 1,000 m^2/g) and similar active functional groups.

A large number of vacant sites were available on the treated activated carbon compared with the untreated activated carbon. The graph shows that at lower initial concentrations (25 and 50 mg/L), the adsorption capacity at equilibrium was 25 and 50 mg/g, respectively (or 100 % removal). At 100 mg/L initial concentration, equilibrium adsorption for CNAC-D3 was almost 100 % (96.47 mg/g) while CNAC-800-3 was succeeded to remove only 73 % or 72.95 mg/g. At this stage, the difference between their pore size and surface area affect significantly the adsorption capacity of both activated carbons.

The equilibrium adsorption for CNAC-D3 was increased from 96.47 mg/g to 381.64 mg/g when the methylene blue initial concentration was increased from 100 mg/L to 500 mg/L compared with the untreated one (from 72.95 mg/g to 348.5 mg/g, respectively). The higher mass transfer for CNAC-D3 was due to the increased in the driving force which was the initial concentration of methylene blue (Ahmad & Alrozi, 2011).

Figure 5.2 exhibits a reverse behavior in the term of percentage removal of methylene blue, as the initial concentration increased from 25 to 500 mg/L, where the graph was plotted in up and down trend. This was due to the fact that the percent removal of methylene blue was decreased from 100 % to 60.54 % from 25 to 300 mg/L, respectively but recorded a slight increased from 400 to 500 mg/L with removal rate of 64.89 to 69.7 %, respectively. This pattern of adsorption indicated the possible monolayer formation of methylene blue on the adsorbent surface (Ahmad & Alrozi,

2011). The percentage of methylene blue removal was lower for CNAC-800-3 compared with CNAC-D3 was due to the lack of available active sites required for further uptake after reaching the equilibrium (Liu et al., 2010).

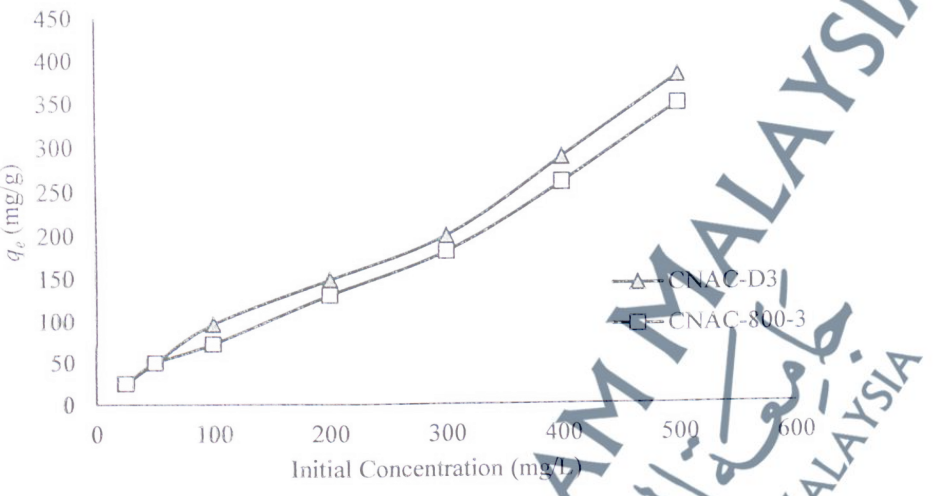

Figure 5.1 Effect of initial concentration on methylene blue removal by acid treated activated carbon.

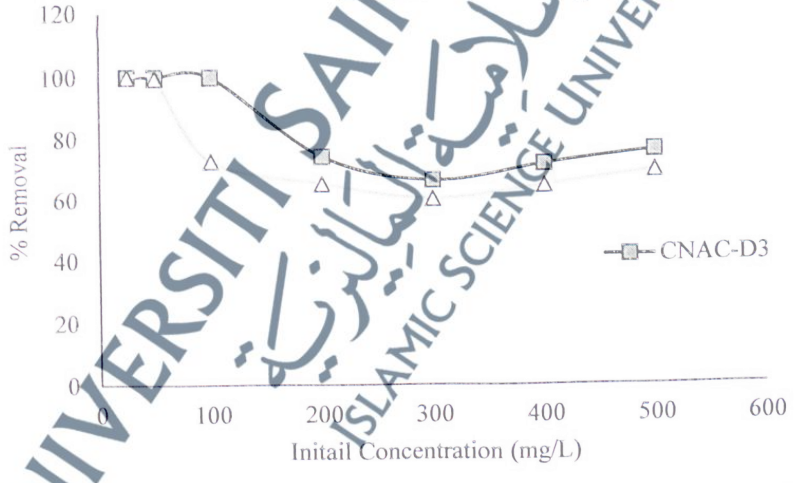

Figure 5.2 Comparison of percent removal on adsorption of methylene blue between CNAC-D3 and CNAC-800-3.

5.4.2 Effect of pH Solution

The effect of pH on removal methylene blue by prepared activated carbon was investigated over a pH range from 2 to 8 and presented as in Figure 5.3. The graph shows the higher removal of methylene blue for CNAC-D3 compared with CNAC-800-3. At pH 5, CNAC-D3 was successful to remove 100 % of methylene blue but CNAC-800-3 was managed to remove 78.05 % of the adsorbate. In fact, at every value of pH, CNAC-D3 adsorbed better.

The patterns for both activated carbons were similar where the percent removal was increased as pH was increased from 2 to 5. Then, the percent removal was decreased when the pH increased from 5 to 8. A relatively similar finding was observed in the previous chapter (Chapter IV: Figure 4.2).

It can be assumed that the pH did not effectively change the adsorption of methylene blue onto the adsorbents (CNAC-800-3 and CNAC-D3). The adsorption capacity was higher in CNAC-D3 was believed to cause by the hydrochloric acid treatment onto the adsorbent, which changed its morphology (Chapter III: Figure 3.12) and the porous structure (Chapter III: Table 3.14). However, the surface functional groups were relatively unchanged (Chapter III: Figure 3.13).

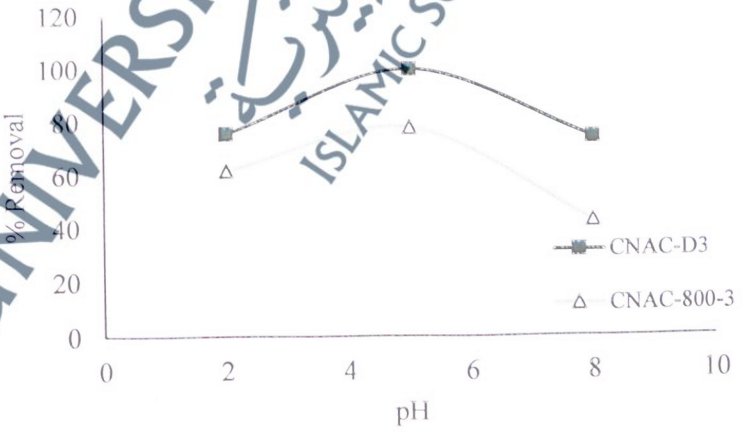

Figure 5.3 The percent removals in CNAC-D3 and CNAC-800-3.

5.4.3 Adsorption Isotherms of Methylene Blue

Figure 5.4 presents the amount of dye adsorbed at the equilibrium time to indicate the maximum adsorption uptake of the cocoa nib-based activated carbon. The adsorption isotherm indicates how the adsorption molecules distribute between the liquid phase and the solid phase when the adsorption process reaches an equilibrium state. It is usually due to the large numbers of vacant surface sites that available for adsorption during the initial stage (Ahmad et al., 2012).

The adsorption equilibrium data were analysed using Langmuir and Freundlich isotherms. Using the linear form of the equations, the methylene blue adsorption equilibrium of Langmuir, Freundlich and Temkin have been successfully plotted as shown in Figure 5.5, 5.6 and 5.7, respectively.

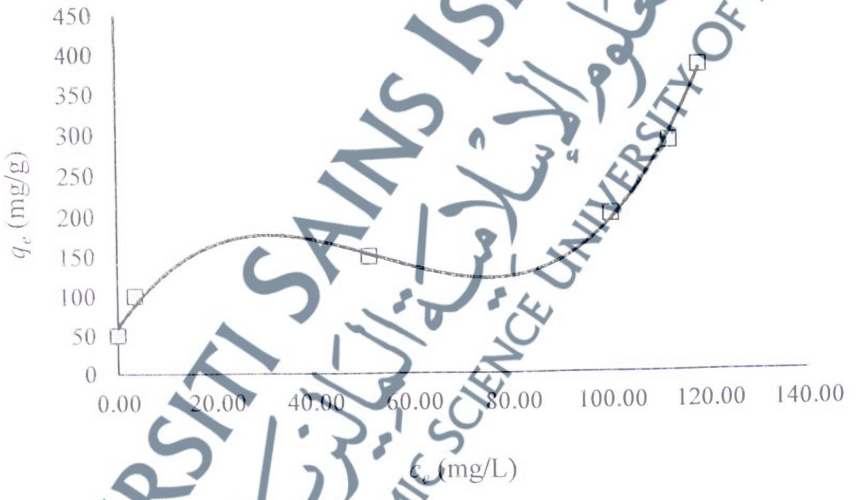

Figure 5.4 Adsorption at equilibrium of methylene blue onto CNAC-D3.

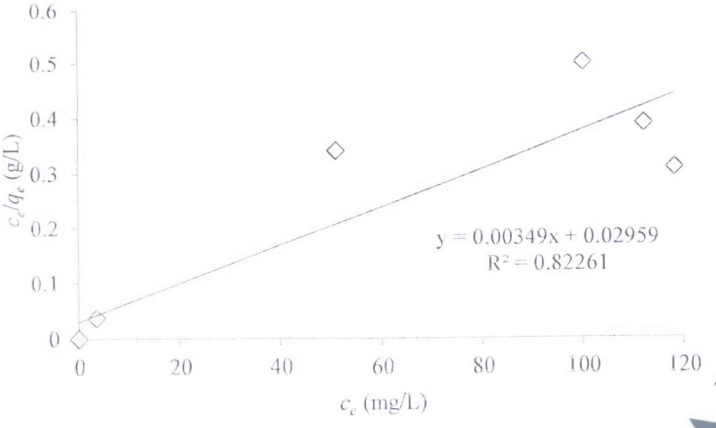

Figure 5.5 Langmuir adsorption of methylene blue onto CNAC-D3.

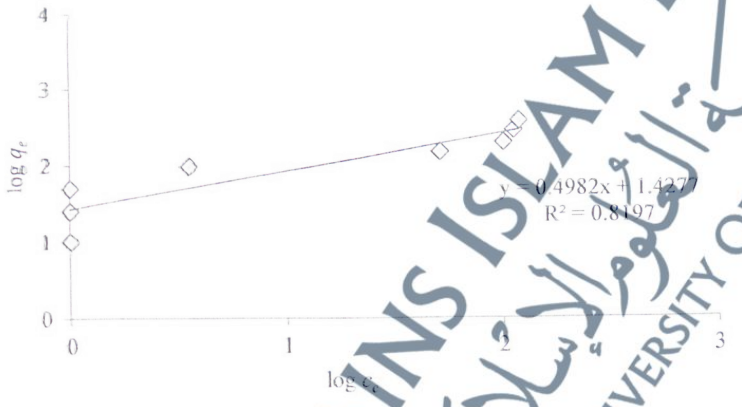

Figure 5.6 Freundlich adsorption of methylene blue onto CNAC-D3.

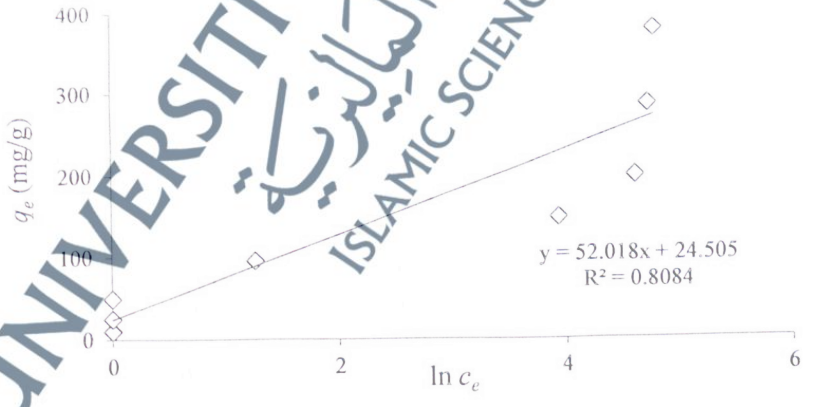

Figure 5.7 Temkin adsorption of methylene blue onto CNAC-D3.

The Langmuir isotherm fits the data well and the correlation coefficient, R^2 values are close to 1. For the Langmuir-type adsorption process, the dimensionless constant, termed as separation factor R_L, is an essential characteristic and has a value of $0 < R_L < 1$, which indicates a favorable isotherm adsorbate/adsorbent as shown in Table 5.1. The R_L value is defined as in equation 5.1.

(5.1) $$R_L = \frac{1}{1+K_L C_i}$$

Table 5.2 summaries the values of methylene blue isotherms constants calculated from the developed plots. A high value of K_L (0.4208 L/mg) and a low value of R_L (0.0232) indicate a high and favorable solute/adsorbent adsorption process (Attia et al., 2008). The values of Langmuir and Temkin constants shown in Table 5.2 indicated a favorable conditions for methylene blue adsorption onto cocoa nib-based activated carbon.

Table 5.1 Separation factor, R_L (Ahmad & Alrozi, 2011)

R_L value	Nature of adsorption process	Calculated R_L value
$R_L > 1$	Unfavourable	x
$R_L = 0$	Linear	x
$0 < R_L < 1$	Favourable	0.0232
$R_L < 1$	Irrevesible	x

Table 5.2 Isotherm constants for adsorption of methylene blue by CNAC-D3

Langmuir	R^2	q_m (mg/g)	K_L (L/mg)	R_L
	0.97634	191.94	0.4208	0.0232
Freundlich	R^2	$1/n$	n	K_f ((mg/g)(mg/L)$^{1/n}$)
	0.7113	0.4556	2.1949	4.2038
Temkin	R^2	A (L/g)	B	-
	0.9381	2.585	34.214	-

Based on Table 5.4, the Freundlich isotherm failed to fit the data well, as the correlation coefficient, R^2 value (0.7113) is far from 1. The fact that the Freundlich isotherm did not fit the experimental data well may be due to a result of homogeneous distribution of active sites onto the CNAC-D3 surface rather than heterogenous distribution. The Freundlich equation represents multilayer and heterogeneous adsorption on the surface of the activated carbon (Argun et al., 2007).

Temkin isotherm assumes that the heat of adsorption of all the molecules in the layer would decrease linearly with coverage due to adsorbent-adsorbate interaction and the adsorption is characterized by a uniform distribution of binding energies, up to some maximum binding energy (Ahmad et al., 2012). A plot of q_e versus ln C_e gives a linear with B as the slope and B ($\ln A_T$) as the intercept, where A_T (L/g) and B are Temkin constants.

Overall, CNAC-D3 showed high adsorption capacity to adsorb methylene blue during the experiments. The relatively high adsorption capacity of methylene blue onto the activated carbon was consistent with the results obtained earlier where the activated carbon are having high surface areas and pore volumes that mainly contribute by mesopores. Besides physical properties, the adsorption capacity of the activated carbon produced were influence by the presence of functional groups such as carboxylic, hydroxyl and nitrile groups on the surfaces. The functional groups could dissociate and became negatively charge sites, which attract the positively charge methylene blue cations in electrostatic interaction (Alrozi, 2010).

Table 5.3 lists a comparison of maximum monolayer adsorption capacity of methylene blue onto several adsorbents. It is clear that cocoa nib-based activated carbon had a relatively moderate adsorption capacity of 191.94 mg/g.

Table 5.3 Comparison of the maximum monolayer adsorption of methylene blue onto various adsorbents

Adsorbent	Maximum monolayer q_e (mg/g)	Reference
Peach stone	412.0	Attia et al., 2008
Ricinus communis epicarp	62.5	Santhi & Manonmani, 2009
Pecan nutshell	400.0	Bello-Huitle et al., 2010
Jatropha curcas fruit shell	499.17	Tongpoothorn et al., 2011
Cocoa shell	212.77	Ahmad et al., 2012
Crescentia cujete fruit shell	66.67	Joseph & Xavier, 2013
Cola nuts hell	87.12	Nsami & Mbadcam, 2013
Fox nutshell	980.39	Kumar & Jena, 2016
Cocoa nibs	191.94	This work

5.4.4 Adsorption Kinetic Studies

The kinetics of adsorption describes the rate of methylene blue uptake on CNAC-D3. The pseudo-first-order and pseudo-second-order kinetic models were applied to evaluate the kinetic parameters of the adsorption process (Agarwal et al., 2015).

Figure 5.8 demonstrates the pseudo-first-order kinetic model to predict sorption kinetics. The values of K_1 and correlation coefficient, R^2 obtained from the plots for methylene blue adsorption on the activated carbon are given in Table 5.6. The experimental q_e values were not in agreement with the calculated values obtained from the linear plots. In addition, the high R^2 (> 0.90) values for methylene blue were not achieved at the lowest concentration (0.812 for 10 mg/L). This shows that the adsorption of methylene blue on the cocoa nib-based activated carbon was not first-order.

Figure 5.9 shows a linear plot of t/q_t versus t to represent the pseudo-second-order kinetic model. This is more likely to predict the behaviour over the whole range of adsorption. The graph shows good agreement between the experimental and the

calculated q_e values, as addressed in Table 5.4. In addition, the correlation coefficient, R^2 values were almost equal to unity (> 0.94) for all methylene blue concentrations, which indicates the applicability of the second-order kinetic model to describe the dye adsorption process on the cocoa nib-based activated carbon.

The results suggest that more than one step may be involved in the adsorption process (Gurses et al., 2006). It also assumes that the rate limiting step is chemical sorption (chemisorption) involving forces created through sharing or the exchange of electrons between sorbent and adsorbate as covalent forces (Ofomaja, 2008).

Figure 5.8 Pseudo-first-order of methylene blue kinetic adsorption.

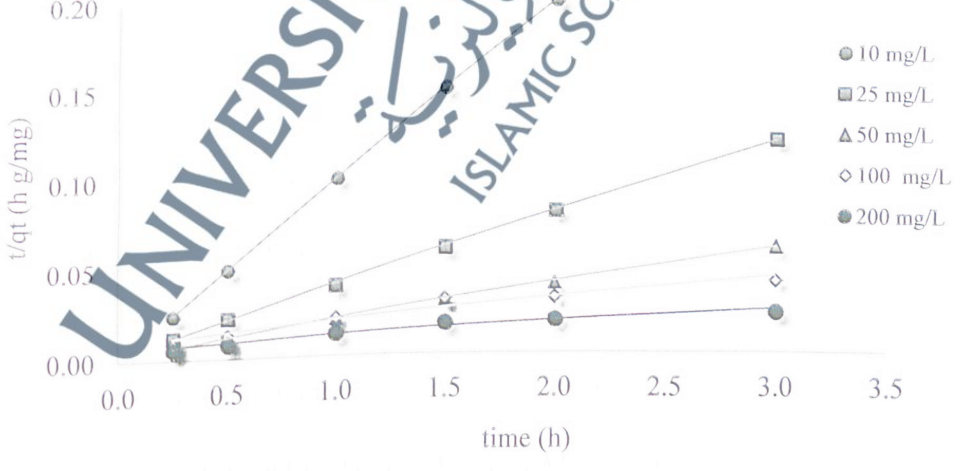

Figure 5.9 Pseudo-second-order of methylene blue kinetic adsorption.

Table 5.4 Adsorption kinetics model equation constants and correlation coefficients for methylene blue adsorption

Initial concentration (mg/L)	Kinetic models					
	Pseudo-first-order			Pseudo-second-order		
	q_e, cal (mg/g)	K_1 (1/h)	R^2	q_e, cal (mg/g)	K_2 (g/mg h)	R^2
10	8.711	15.369	0.812	10.000	0.000	1.000
25	19.508	4.081	0.916	25.641	0.691	0.995
50	43.654	3.087	0.963	52.356	0.159	0.995
100	83.188	0.390	0.963	87.719	0.014	0.942
200	160.871	0.397	0.969	158.730	0.007	0.945

5.4.5 Adsorption Mechanism

The mechanism of adsorption was predicted using the adsorption and kinetic isotherm. This is to characterize the solid-liquid sorption process, whether it is external mass transfer (boundary layer diffusion) or intra-particle diffusion or both (Klaewkla, 2011). The effect of intra-particle diffusion resistance on adsorption can be determined by the equation 5.2.

(5.2) $$q_t = K_{id}t^{1/2} + C_i$$

where K_{id} is the intra-particle diffusion rate constant (mg/gmin$^{1/2}$).

Figure 5.10 shows a plot of q_t against $t^{1/2}$, derived from Equation 5.12 to give a linear plot with slope k_{id} and intercept C_i. The C_i value provide the information on the thickness of the boundary layer where the larger the value, the greater the contribution of the surface sorption in the rate-controlling step (Dülger et al., 2013).

A different nature of the plotted graphs was obtained due to the wavering of sorption at the initial stage and at the final stage of the adsorptions. This phenomenon can be due to boundary layer diffusion which occurred at the initial stage and the intraparticle diffusion which occurred in the later stage (Kumar et al., 2011).

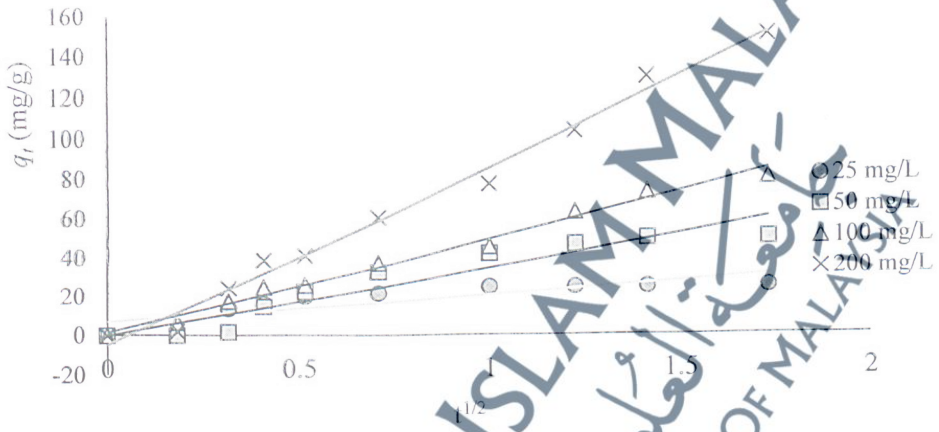

Figure 5.10 Intraparticle diffusion of methylene blue adsorption onto CNAC-D3.

It can be observed from the graph that the linear line for 50 mg/L and 100 mg/L of initial concentration of methylene blue passed through the origin (0), but the other two (25 mg/L and 200 mg/L) were not. The linear regression of the plot that passed through the origin indicating an intraparticle diffusion as its rate-limiting step. The linear plots that failed to pass through the origin were assumed to be due to the difference in the rate of mass transfer in the initial and final stages of adsorption. This pointed out that rate-limiting step was not only the intraparticle diffusion but together with the boundary layer control, which can be operating simultaneously in the sorption process (Kumar et al., 2011).

Figure 5.11 shows the calculated B_t values were plotted against time (t; hour). The q_e for 25, 50, 100 and 200 mg/L was 25, 50, 99.25 and 181.25 mg/g, respectively. The calculated F and B_t values were listed as in Table 5.5. These values were used to

develop linear plot in order to identify whether external transport or intra-particle transport controlled the rate of adsorption (Benaissa, 2010).

Linear lines were obtained in Figure 5.11, however every line developed did not pass through the origin. According to Kumar et al. (2011), if the linearity was achieved and the line passes through the origin, it indicates the internal diffusion is the slowest step in the adsorption process. From Figure 5.11 too, it was observed that linearity that was plotted did not pass through the origin. This situation indicated that film diffusion had influence on the adsorption process too (Kumar et al., 2011; Benaissa, 2010).

Table 5.5 Calculated values for F and Bt

	25 mg/L		50 mg/L		100 mg/L		200 mg/L	
t (hour)	F	B_t	F	B_t	F	B_t	F	B_t
0	0	-0.4977	0	-0.4977	0.0000	-0.4977	0.0000	-0.4977
0.25	0.6924	0.6813	0.531	0.2595	0.2635	-0.1919	0.2236	-0.2446
0.5	0.8752	1.5833	0.8484	1.3888	0.3807	-0.0186	0.3357	-0.0887
1	-	-	0.9392	2.3025	0.4622	0.1225	0.4269	0.0590
1.5	-	-	0.984	3.6375	0.4832	0.1624	0.4677	0.1329
2	-	-	-	-	0.6383	0.5192	0.5717	0.3503
3	-	-	-	-	0.7402	0.8500	0.7149	0.7571

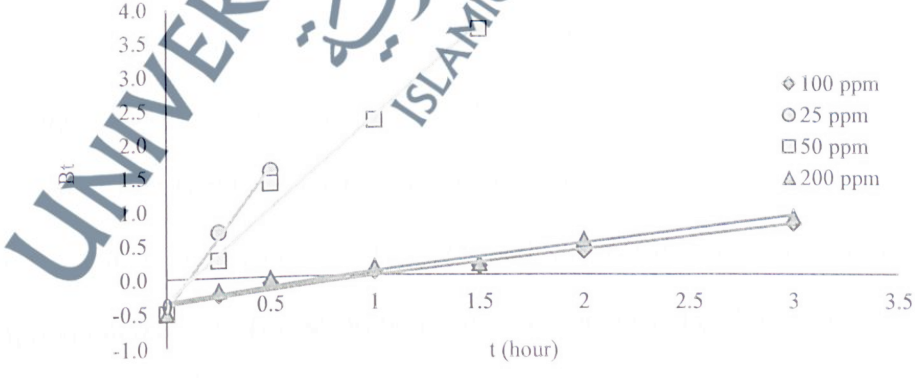

Figure 5.11 Boyd plot for adsorption of methylene blue onto CNAC-D3.

As the adsorption of methylene blue onto the treated CNAC was controlled by film diffusion, external transport is shown to be more prominent than internal transport. This system indicates the operation of two stages: external mass transfer during the initial sorption process followed by intraparticle diffusion of methylene blue onto acid treated cocoa nib-based activated carbon. Film diffusion is usually rate limiting in systems that have small particle size and high adsorbate affinity for the adsorbent (Ahmad et al., 2012). Similar observations were obtained by Ahmad et al. (2012), Kumar et al. (2011) and Benaissa (2010) in adsorption of methylene blue onto cocoa shell, cashew nut shell and almond peel-based activated carbon, respectively.

5.5 Conclusion

From these results, it is seen that the pseudo-second-order kinetic model and Boyd model are applicable for this adsorption system. The applicability of both models showed that the adsorption process is complex which involves more than one mechanism (Ahmad et al., 2012; Benaissa, 2010).

The pseudo second-order equation provided better fit and a good linearization with R^2 (>0.999) for most of the systems (Table 6.5), a conclusion that is further strengthened by the Langmuir isotherm equation and the Boyd model. Therefore, it is safe to assume that adsorption is likely to follow chemisorption. This assumption is also based on the observation by Ahmad et al. (2012) and Bulut et al. (2008).

The adsorption (chemisorptions) might take place until the surface active sites are fully occupied. Then, the methylene blue molecules diffuse into the pores for further adsorption interactions. The adsorption capacity of activated carbon is thus dependent not only on the surface area but also on the interaction of positive ions with surface functional groups of activated carbon.

The adsorption of methylene blue on cocoa nib-based activated carbon followed the Langmuir and Temkin isotherm models ($R^2 > 0.9$). The pseudo-second-order kinetic model and Boyd model fits for the adsorption. The monolayer adsorption (191.94 mg/g) capacity was comparable with other adsorbents (Table 6.3). The pseudo-second-order model fits better for the adsorption kinetics as compared to the pseudo-first-order model. The adsorption kinetic models suggest the adsorption process is complex, involving more than one mechanism. The mechanism may involve adsorption of dye at an active site on the surface, diffusion and adsorption into the interior pores of the activated carbon particles. The results of this study show that the activated carbon produced from cocoa nibs and treated with hydrochloric acid can be used as potential adsorbent in methylene blue removal in aqueous solution.